Calcium and Potassium in the Motor Organ of the Sensitive Plant: Localization by Ion Microscopy

Abstract. *The ion microscope was used to study potassium and calcium distributions in the main motor organ of* Mimosa pudica *L. The cortex of the motor organ has two cell types differing in location, structure, and ion distribution. Histochemical features portrayed in ion micrographs were plainly correlated with structures seen in the light and electron microscopes.*

The transport and compartmentalization of inorganic ions are important factors in a variety of biological phenomena. Accordingly, there is a great interest in techniques for localizing ions in cells and tissues. Although noteworthy findings about elemental composition have resulted from the use of electron microprobe x-ray analyses (*1*), point-by-point mapping of an element's distribution can be tedious. The Cameca IMS-300 ion microscope is designed with unique ion optics that allow direct microscopic imaging and thereby maintain a one-to-one correspondence between the lateral distribution of the ions on the sample surface and that of the final mass-resolved ion image. This resultant image has a spatial resolution of 1 μm and a field diameter of about 250 μm. As an alternative to the electron probe, the ion microscope offers the advantage of providing a more obvious "fit" of an element's distribution to a tissue's anatomy (*2*). In addition, it has much greater sensitivity and is capable of detecting all elements of the periodic table. Although the sensitivity for a particular element depends on the nature of the element, its chemical form, and the matrix in which it is located, the instrument is generally most sensitive for the lighter elements.

The ion images in this study were produced by bombarding the sample with an O_2^+ primary beam at an energy of 5.5 keV and a beam density of approximately 10^{-5} A/cm^2. The secondary ions emitted from the surface were focused and accelerated to the entrance slit of a double-pass magnetic sector for momentum filtering. An electrostatic mirror positioned after the first pass of the magnet allows the ion beam to be energy filtered. Thus a mass spectral analysis of the ions present within the areas of interest may be obtained. The secondary ion image, which is subsequently converted to an electron image by a Cu-Be cathode, may be (i) projected onto a fluorescent screen for viewing and survey, (ii) projected onto electron-sensitive film for permanent recording, or (iii) directed to a scintillator-photomultiplier detector system for ion counting over a preselected area or feature in the ion image (*3*).

Although a few ion microscopic studies of animal tissues have been reported (*4*), we do not know of any application of ion microscopy for the investigation of a plant tissue. In this report we describe ion microscopic observations of the main pulvinus (motor organ) of the sensitive plant.

The leaves of *Mimosa pudica* L., the sensitive plant, respond to touch and other stimuli with rapid (< 1 second) movements. These leaf movements result from the curvatures of specialized motor organs, the pulvini. The pulvinar curvatures occur when motor cells in opposing regions of the pulvinus differ in turgor (*5*). This requires accumulation and loss of water by the motor cells, and it is likely that this water movement is an osmotic consequence of redistribution of potassium ions within the pulvinus (*6*). The response and recovery of pulvini are also associated with relocation of calcium ions in the motor tissue, although the function of this Ca^{2+} movement is not known (*7*). We have used the ion microscope to localize potassium and calcium within the main pulvinus. Greenhouse-grown plants were placed in a bright, 3°C cold room for 2 hours before sample preparation. Under such cold conditions, the petioles recover to the elevated (unstimulated) position and are insensitive to stimulation. Such cold-anesthetized plants are therefore a

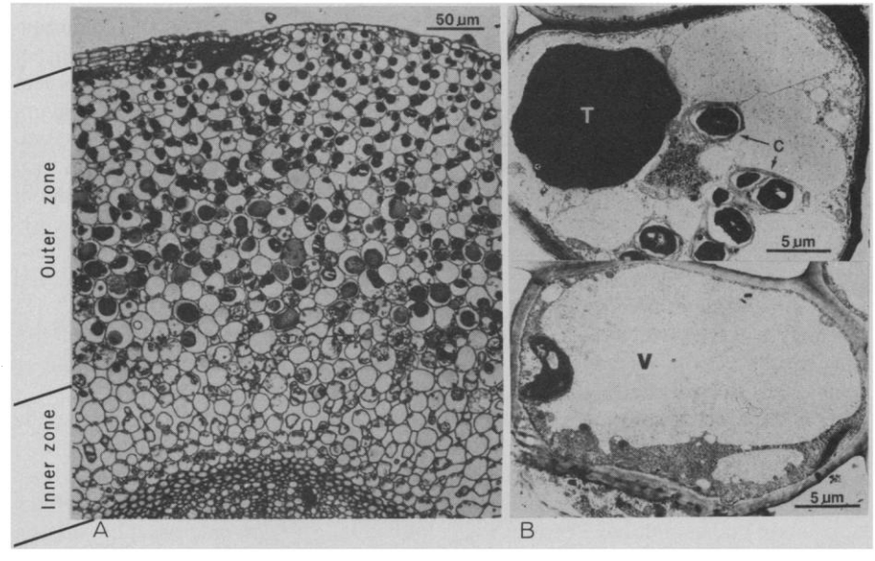

Fig. 1. (A) Light micrograph of the abaxial (lower) side of the main pulvinus of *Mimosa*, showing two zones of cortex. Vein is at the bottom, epidermis at the top. (B) Electron micrographs of a typical outer zone cell (top) and an inner zone cell (bottom). *T*, tannin body; *C*, chloroplast; and *V*, central vacuole.

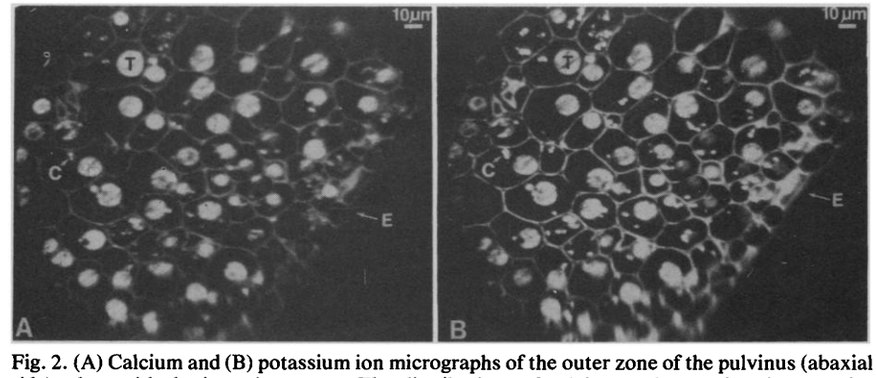

Fig. 2. (A) Calcium and (B) potassium ion micrographs of the outer zone of the pulvinus (abaxial side) taken with the ion microscope. The distributions of calcium and potassium ions are indicated by the bright areas in the photographs. Although ion microscopic analysis is a destructive technique, these two photographs are of essentially the same depth in the sample since exposure times are only a few seconds while the sputter lifetime of the these 300-mm sections is 30 minutes. *T*, tannin body; *C*, chloroplast; and *E*, epidermis.

0036-8075/79/0413-0185$00.50/0

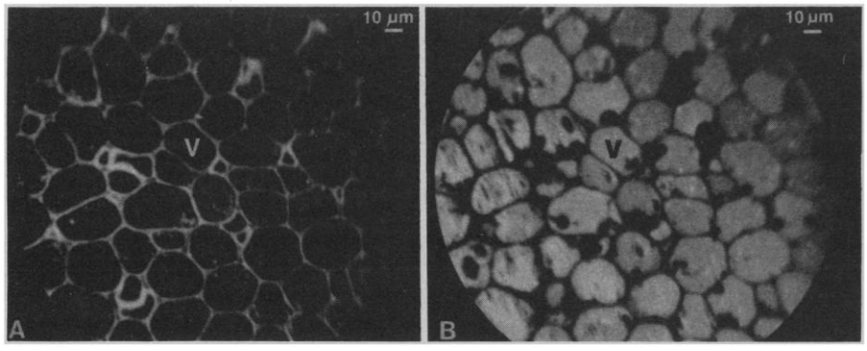

Fig. 3. (A) Calcium and (B) potassium ion micrographs of the inner zone of the pulvinus (same field for both photographs). *V*, central vacuole.

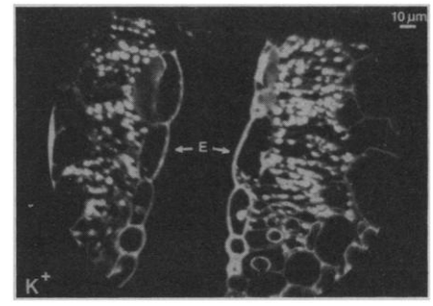

Fig. 4. Potassium ion micrograph of two opposing *Mimosa* leaves. Beneath the epidermis (*E*) is palisade mesophyll with very bright chloroplasts, indicating an abundance of K^+.

source of unstimulated pulvini. The main pulvini, which attach the petioles to the stem, were excised, fixed in glutaraldehyde and osmium, and dehydrated in acetone (*8*). Fixation and dehydration were conducted at 3°C. After fixation and dehydration the pulvini were still in the unstimulated conformation. After embedding in Spurr's plastic (*9*), the samples were sectioned for light, electron, and ion microscopy (*10*). We are aware of the problem of loss and redistribution of ions during chemical fixation (*11*). However, in this initial study our primary concern was preservation of structure, since we were trying to generate ion micrographs with well-defined histological detail.

The main pulvinus of *Mimosa* is a cylinder consisting of a central vein surrounded by a thick cortex of motor cells. This cortical region has two distinct concentric histological zones (Fig. 1). The outer zone is characterized by cells with large tannin bodies, which have been described in detail by Toriyama (*6*). Most cells in the inner zone (near the vein) lack tannin bodies, but have central vacuoles generally containing a matrix material.

Ion micrographs of the outer zone indicated that the tannin bodies, plastids, and cell walls were relatively rich in both potassium and calcium (*12*) (Fig. 2). However, in the inner zone K^+ and Ca^{2+} were segregated (Fig. 3). Calcium was abundant in the cell walls but scarce within protoplasts. Conversely, K^+ was absent from the walls but plentiful in the central vacuole and (possibly) the cytoplasts.

Since the cells of the two zones of the main pulvinus differ both in structure and in the distribution of key ions, we suspect that these two cell types also differ in function. The possible role of the tannin bodies of *Mimosa*'s motor cells has been the focus of considerable investigation (*13*). The tannin bodies change size and shape during pulvinar response and recovery (*14*). Toriyama and Jaffe (*7*) localized Ca^{2+} in the main pulvinus by staining formalin-fixed tissue with alizarin red sulfate. Their findings suggested loss of Ca^{2+} from the tannin bodies during pulvinar response and reabsorption of Ca^{2+} by the tannin bodies during recovery. Toriyama and Jaffe proposed that redistribution of Ca^{2+} could affect leaf movements by inducing conformational changes of contractile proteins. It is more likely that calcium affects leaf movements by directly altering membrane permeabilities (*15*). Our observation, by ion microscopy, that the tannin body has a high calcium content corroborates Toriyama and Jaffe's hypothesis that the tannin body functions as a Ca^{2+} reservoir. Since we observed that the tannin body is also a K^+-rich site, it is probable that the role of this structure in rapid leaf movements is complex.

The absence of tannin bodies in the cells of the inner zone may be one structural indication of a functional difference between the two cortical zones of the pulvinus. Our ion micrographs suggest that K^+ is abundant in the inner cells. Considering their location and their high K^+ content, the cells of the inner cortex could be important in regulating K^+ content and turgor of the motor cells of the outer cortex. Another interesting difference between the inner and outer zones was the abundance of K^+ in the walls of the outer cells and the virtual absence of K^+ in the walls of inner cells. Regardless of whether this represents the situation in vivo or is an artifact of sample preparation, it suggests that the two zones differ in cell wall chemistry. Since the outer cells, but not the inner cells, undergo very large volume changes during pulvinar bending (*16*), some specialization of cell wall chemistry in the outer zone is likely.

The degree to which the distribution of ions we observed in the pulvinus reflects the situation in vivo may be debatable. During fixation, there should be ample opportunity for loss and relocation of diffusible ions. We are especially skeptical about the K^+ localization since this ion is largely in an unbound state in plant tissue (*17*). In fact, only 22 ± 4 percent of the pulvinar K^+ was retained during our sample preparation (*18*). We are considerably more confident about the observed distribution of calcium. It is likely that Ca^{2+} in most plant tissue is largely immobile (*17*). Consistent with this, we found that nearly all (92 ± 3 percent) of the Ca^{2+} of the pulvinus remained after fixation and dehydration. Apparently, extensive redistribution of the potassium and calcium that does remain in the fixed tissue is somehow impeded. The ion micrographs have considerable structure and do not show randomization of ions. For instance, K^+ ion micrographs of *Mimosa* leaves show chloroplasts as structures with a high K^+ content (Fig. 4). This is consistent with evidence that chloroplasts have a high K^+ concentration in vivo (*19*).

This inaugural application of ion microscopy for the study of plant tissue is encouraging. The distribution of ions over large areas of tissue was rapidly surveyed and structural features on the ion micrographs were easily correlated with those on light and electron micrographs. These attributes make iron microscopy an attractive supplement to the study of plant cells by electron probe–x-ray analysis.

NEIL A. CAMPBELL
Section of Botany, Genetics, and Development, Cornell University, Ithaca, New York 14853
KATHERINE M. STIKA
GEORGE H. MORRISON
Department of Chemistry, Cornell University

References and Notes

1. T. A. Hall, in *Microprobe Analysis as Applied to Cells and Tissues*, T. Hall *et al.*, Eds. (Academic Press, London, 1974), p. XV.
2. G. H. Morrison and G. Slodzian, *Anal. Chem.* 47, 932A (1975).
3. For more on the theory of the instrument, see P.

Galle, in *Microprobe Analysis as Applied to Cells and Tissues*, T. Hall *et al.*, Eds. (Academic Press, London, 1974), p. 89.
4. A. Y. Jeantet, R. Martoja, M. Truchet, *C. R. Acad. Sci. Ser. D* **278**, 1441 (1974).
5. R. Aimi, *Bot. Mag.* **73**, 412 (1960).
6. H. Toriyama, *Cytologia* **20**, 367 (1955).
7. _____ and M. J. Jaffe, *Plant Physiol.* **49**, 72 (1972).
8. Fixation was for 5 hours in 3 percent glutaraldehyde (sodium phosphate-buffered, *p*H 7.1), postfixation for 3 hours in 1 percent phosphate-buffered OsO_4.
9. A. R. Spurr, *Bot. Gaz. (Chicago)* **133**, 263 (1972).
10. Thick sections for light microscopy were stained with toluidine blue. Thin sections for electron microscopy were stained with uranyl acetate and lead citrate and viewed on a Philips EM 300 at 60 kV. Sections for ion microscopy were 300 to 400 nm thick.
11. P. Echlin and R. Moreton, in *Microprobe Analysis as Applied to Cells and Tissues*, T. Hall *et al.*, Eds. (Academic Press, London, 1974), p. 159.
12. Although the distributions of K^+ and Ca^{2+} in the sample are being analyzed, the mass spectrometer is used to record the most intense secondary ion signals produced. These are the masses of the most abundant singly charged isotope of these elements, $^{39}K^+$ and $^{40}Ca^+$.
13. H. Toriyama, *Proc. Jpn. Acad.* **43**, 777 (1967).
14. _____ and Y. Komada, *Cytologia* **36**, 690 (1971).
15. N. A. Campbell and W. W. Thomson, *Plant Physiol.* **60**, 635 (1977).
16. _____, *Ann. Bot.* **41**, 1361 (1977).
17. A. Nason and W. D. McElroy, in *Plant Physiology*, F. C. Steward, Ed. (Academic Press, New York, 1963), vol. 3, p. 451.
18. The K^+ and Ca^{2+} contents of fixed and dehydrated pulvini were compared to those of pulvini taken directly from a plant. After acid digestion, ion determinations were by atomic absorption spectrophotometry. The ion content of the unfixed pulvini was 275 ± 15 mmole/kg (fresh weight) for K^+ and 65 ± 7 mmole/kg (fresh weight) for Ca^{2+}.
19. A. W. D. Larkum, *Nature (London)* **218**, 447 (1968).
20. Supported by NIH grant GM 24314-01.

10 October 1978; revised 18 December 1978

Uncoupling Agents Distinguish Between the Effects of Metabolic Inhibitors and Transport Inhibitors

Abstract. *In studies with toad bladders, the uncoupling agent 2,4-dinitrophenol (DNP) reversed the inhibition of CO_2 production produced by direct inhibition of transport. In contrast, DNP did not reverse the inhibition of CO_2 production brought about by metabolic inhibitors. Therefore, the response to DNP distinguished between inhibition of transport and metabolism; this approach may be useful for the investigation of factors that regulate active transport.*

In many biological systems the processes of energy production by metabolic pathways and energy utilization vary in a parallel fashion—that is, metabolism and biological work are tightly coupled. This is because the rate of oxidative phosphorylation (and glycolysis) is regulated by the availability of adenosine diphosphate (ADP), a phenomenon termed "respiratory control" (*1*). The close relationship between energy production and energy utilization has made it difficult to elucidate the mechanism of action of factors that influence these processes. In the case of active transport, the hormones aldosterone and thyroxine have been shown to stimulate metabolism (*2*) and transport (*3*). Similarly, diuretic drugs have been shown to inhibit metabolism (*4*) and transport (*5*). Because metabolism and transport are tightly coupled, the primary mechanism of action of these agents remains controversial.

In the present experiments, the uncoupling agent 2,4-dinitrophenol (DNP) was used to distinguish between agents that directly inhibit transport and agents that directly inhibit metabolism. Uncoupling agents have the ability to stimulate respiration when ADP is rate-limiting (*6*). Therefore, if active transport is directly inhibited, respiration would be diminished secondarily, because of reduced adenosine triphosphate (ATP) utilization and ADP production; in this case, DNP would be expected to restimulate respiration. In contrast, if metabolism is directly inhibited, DNP would not be expected to restimulate respiration.

Experiments were performed with urinary bladders of toads (*Bufo marinus*) obtained from the Dominican Republic. Hemibladders were mounted in chambers and continuously voltage clamped. The short-circuit current (SCC) of these bladders is an accurate measurement of active sodium transport (*7*). The rate of CO_2 production (QCO_2) by the bladder was continuously monitored by a method using differential conductivity (*8*). Each bladder was divided into an experimental and a control hemibladder. The SCC and QCO_2 of control hemibladders declined slightly during the 2-hour experiment. After a 1-hour baseline measurement period, an inhibitor was added to the experimental hemibladder. Continuous monitoring of SCC and QCO_2 indicated that a new steady state was reached in 45 to 60 minutes. At this time $10^{-5}M$ DNP (shown in dose-response experiments to be maximally effective) was added to both the control and experimental hemibladders. The peak QCO_2 after the addition of DNP was then recorded.

The results are shown in Table 1. Direct inhibition of active transport either by removal of sodium from the bathing solutions (and substitution with choline) or by the addition of $10^{-3}M$ ouabain (which markedly inhibits active sodium transport) significantly inhibited the SCC and lowered the QCO_2. The subsequent

Table 1. Effects of transport and metabolic inhibitors and DNP on QCO_2 of toad bladders. The data are expressed as means ± standard error. The short-circuit current (SCC) was measured in microamperes; CO_2 production (QCO_2) was measured in microliters per hour. Na^+ removal was accomplished by substituting choline in the Ringer solutions for Na^+. The *P* values indicate whether the change in QCO_2 produced by DNP was significant; NS, not significant.

Type of inhibition	Baseline values		After inhibition		After addition of $10^{-5}M$ DNP		Change produced by DNP	
	SCC	QCO_2	SCC	QCO_2	SCC	QCO_2	QCO_2	*P*
Inhibition of transport								
Na^+ removal ($N = 8$)*	170 ± 34	22 ± 3	7 ± 7	12 ± 2	5 ± 5	23 ± 3	11	<.01
Ouabain ($1 \times 10^{-3}M$) ($N = 13$)	203 ± 54	40 ± 4	75 ± 59	33 ± 4	2 ± 1	78 ± 8	45	<.001
Inhibition of metabolism								
Antimycin A ($1 \times 10^{-5}M$) ($N = 9$)	185 ± 38	31 ± 7	46 ± 9	16 ± 6	15 ± 5	16 ± 6	0	NS
Rotenone ($1 \times 10^{-5}M$) ($N = 10$)	144 ± 26	22 ± 2	55 ± 8	12 ± 1	20 ± 3	13 ± 2	1.0	NS

*N is the number of hemibladders.

0036-8075/79/0413-0187$00.50/0